PHASE STABILITY AND MORPHOLOGICAL EVOLUTION OF HYDROXYAPATITE PREPARED AT DIFFERENT BALL-MILLING TIME

R.M.S. Raja Muhamad Ghouse[1], A.N. Natasha[1,2*], C.M. Mardziah[1,2], N.F. Shahedan[1] and L.T. Bang[3]

[1]Faculty of Mechanical Engineering,
Universiti Teknologi MARA (UiTM), 40450 Shah Alam, Selangor, Malaysia.

[2]Engineered Materials and Structures Research Group,
Faculty of Mechanical Engineering, Universiti Teknologi MARA,
40450 Shah Alam, Selangor, Malaysia.

[3]School of Materials Science and Engineering, Hanoi University of Science and Technology, No. 1 Dai Co Viet, Hai Ba Trung, Hanoi, Vietnam.

*Corresponding Author's Email: natashanawawi@uitm.edu.my

Article History: Received 3 December 2024; Revised 12 September 2025; Accepted 18 October 2025

ABSTRACT: Eggshells are readily available organic wastes used as calcium precursors in the form of calcium oxide for producing Hydroxyapatite (HA). However, limited research has been reported on the potential of eggshell-derived calcium precursors in calcium carbonate ($CaCO_3$). This study used $CaCO_3$ from calcined eggshell waste as a sustainable calcium precursor to synthesise HA by combining mechanochemical activation and a heat treatment regime at 800 °C. The effects of varying ball milling duration (5, 6, and 7 hours) at the rotational speed of 550 rpm were explored. It was observed that all synthesised powders exhibited a high degree of HA crystallinity with a minor appearance of β-TCP as the milling time increased from 6 to 7 hours. Better crystallite size with increased milling times was observed with 16.15nm, 12.767nm and 12.237nm for 5,6 and 7 hours of ball-milling time, respectively. A similar trend was also exhibited in morphological analysis whereby the agglomeration of particles along with average particle size decreases with milling times. Besides that, the Ca/P ratio obtained in all synthesised powders closely resembles the Ca/P ratio of pure HA at 1.67. Thus, $CaCO_3$ from calcined

eggshell waste has been successfully employed as a sustainable calcium precursor in producing eggshell-derived HA.

KEYWORDS: *Eggshells; Calcium Carbonate; Hydroxyapatite; Ball Milling Times; Sintering*

1.0 INTRODUCTION

In modern engineering applications of industrial technology, the harnessing of biomaterials for medical applications [1] has been widely used, especially in bone grafts and dental implants. Numerous approaches have been explored to obtain hydroxyapatite (HA) by synthesising it through various processes such as the sol-gel method [2], wet chemical method [3], hydrothermal [4], combination method, microemulsion method [5] and spray pyrolysis method [6-7]. In complex tissue engineering, calcium phosphates are widely used and favoured in bone graft applications due to their lightweight, stable, and other properties comparable to and similar to the natural bone phase. Previous research has shown that calcium phosphates consist of ions similar to human bones, making the calcium phosphates highly compatible [8], [9]. HA is the predominant crystalline phase of calcium phosphate, which can be found in teeth and bones as the primary mineral constituent [10-12]. Due to its inherent limitations in mechanical strength, most of the bioceramic research focuses on enhancing the mechanical and biological properties of current bioactive ceramics, especially HA.

HA powder, due to its osteoconductive and biocompatible properties, is fundamental in developing bioceramics materials with diverse applications in the medical field. One notable application is for cancer treatment. HA can be a carrier for the targeted delivery of radioactive isotopes using glass beads [13]. Beyond its usefulness in medical applications, HA has also been found to be helpful in environmental remediation. The ability of HA to remove heavy metals in soil treatment and wastewater purification could contribute widely to environmental sustainability [14]. The excellent and exceptional biocompatibility and osteoconductivity of HA are the principal factors and main reasons why studies regarding HA have been made thoroughly [9]. Due to patients' movement being limited during bone injury as bone's ability to self-repair is also limited, tissue engineering has emerged with the idea of promoting bone regeneration [12], [15]. This approach involves generating and manipulating tissue growth in

a laboratory setting to replace damaged tissues within the body [12], [13]. Prominent research has demonstrated that the incorporation of HA significantly enhances surface roughness, promoting improved cell adhesion and proliferation [16]. HA has reportedly increased the healing rate due to a more intimate attachment between implant HA and the natural bone [17]. This potential of HA in repairing bone defects is the main reason HA is widely used in medical applications.

Considering the wide and various range of applications of HA, especially in biomedical fields, the diverse and numerous number of synthesis methods are currently concerning. Prior research on various methods has been conducted to obtain HA from eggshell waste, resulting in low and high-purity grades of powder eggshells. Past research has also utilised the precipitation method along with calcium oxide as a calcium precursor from the limestone [18]. However, calcium oxide has high reactivity and potential for impurities. Researchers are seeking the most simple and cost-effective technique for synthesising HA while providing vital properties, features, and characteristics for specific fields and applications [19]. Research was done by S. Ramesh et al. [20-22] through a dry method that utilises attrition milling and calcium carbonate ($CaCO_3$) as the calcium precursor. The method used had successfully produced HA that is close to pure HA. This finding shows that the dry synthesise method is reliable. However, the available attrition milling method is high and energy-consuming.

Hence, an appropriate mixing method is needed to obtain the properties needed for specific applications. Other than that, the temperatures of the synthesising method will affect the crystallinity, purity, morphology and topography of acquired HA.

In addition, the duration of the ball-milling process can crucially affect the phase stability and morphology of HA obtained from a mixture of DCPD and calcined eggshells. As the milling process time increases, the mechanical energy input contributes to the reduction of particle size, potentially enhancing the HA's stability by increasing the surface area of the particles [23]. Thus, this research aims to determine the effect of ball-milling times on the phase stability and morphology of HA synthesised via solid-state reaction using $CaCO_3$ from eggshells as a sustainable calcium precursor.

2.0 METHODOLOGY

2.1 Materials

The primary material used in this research is chicken eggshell, which is the primary source of calcium, Ca. The eggshells were collected from a restaurant at Management & Science University (MSU) Seksyen 13, Shah Alam. The primary source of phosphate comes from the Dicalcium Phosphate Dihydrate (DCPD), purchased from Naqalai Tesque, Kyoto, Japan.

2.2 Synthesis of Hydroxyapatite (HA)

Chicken eggshells were used as the primary source of calcium in the form $CaCO_3$, while Dicalcium Phosphate Dihydrate (DCPD) was utilised as the primary phosphate source. The raw chicken eggshells were collected from a restaurant at MSU Sexyen 13, Shah Alam. The collected eggshells were washed using distilled water, removing the membrane and dirt around them. The eggshells were then dried at 110°C for 24 hours in a drying oven.

The dried eggshells were then crushed using a pestle and mortar to obtain eggshell powder. In addition, to ensure the size of the powders was uniform and homogenous, the crushed powders were sieved using a 250-mesh sieve. Thermogravimetric Analysis (TGA) was done on the raw eggshell powder with powder mixture of DCPD and calcined eggshell to determine the suitable temperature for the calcination and sintering process. The crushed eggshell powder was finally calcined at 700°C for 2 hours with a heating rate of 5°C/min using a thermolyne furnace to obtain pure $CaCO_3$

The synthesis of HA powder was done using the mechanochemical method, which combines ball-milling and sintering methods. The ball-milling method mixed the calcined eggshell and DCPD with the parameters of 550 rpm and various times of 5,6 and 7 hours. The parameters were determined with the help from our previous study and the orthogonal array method which is L3, that is equal to 3^1. The mixing of the calcined eggshell and DCPD was done at a Ca/P ratio of 1.67. After completing mixing in the ball mill, the mixture was sintered in a thermolyne furnace at 800°C for 5 hours with a heating rate of

5°C/min to obtain the HA powder.

2.3 Characterization of Synthesised Powder

All the synthesised powder samples were labelled as follows for characterisation and comparison purposes.

Table 1: Sample parameters

Sample	Milling Parameters
S1	550 rpm – 5 hours
S2	550 rpm – 6 hours
S3	550 rpm – 7 hours

2.3.1 X-Ray Diffraction Analysis (XRD)

X-ray X-ray diffractometer (XRD) was utilised to analyse the crystal structure of all the samples that underwent ball-milling at different mixing times. All the samples went through the X-ray diffraction (XRD) analysis by using Rigaku (Model D-Max-2200) to observe the crystallite size and phase composition of the sample [24]. The XRD was run at 40kV and 40mA. The scanning speed used for the test was constant for all samples at 2°/min. Despite the longer time taken for each test compared to higher scanning speeds, the detail of each peak was better in terms of intensity. In addition, the weaker peaks could also give better identification that could be overlooked if a higher scanning speed was used. The samples were scanned in 2θ with a range of 10° to 90°. The XRD result was plotted using Origin8Pro and analysed using Profex V5.2.9. The Profex helps to identify phases that exist in the obtained HA powder. The crystallite size was calculated based on three main planes peaks of HA, which are (211), (112) and (300), via Scherrer's equation as follows:

$$D = \frac{k\lambda}{\beta \cos \theta} \quad (1)$$

2.3.2 Fourier Transform Infrared Spectroscopy (FTIR)

Fourier Transform Infrared Spectroscopy (FTIR) was used to analyse the characteristic vibrational frequencies of different functional groups that are present in the synthesised compound. For HA compounds, phosphate, hydroxyl and carbonate are the main functional groups that

should exist in the analysis.

2.3.3 Scanning Electron Microscopy (SEM)

The morphology of the synthesized powder at different ball milling times was examined using a scanning electron microscope (SEM). The powder samples were coated with gold using nano sputter carbon, and random spots were randomly chosen to examine the samples' elements and observe the samples' morphology. The equipment used was the Carl Zeiss Microscopy (Model EVO 18). The magnification of the SEM was 5000X and 10000X. The average particle size was also determined by using the line intercept method. Besides that, the Energy Dispersive X-ray (EDX) was run along random spots on each sample to examine the composition presence in the samples.

3.0 RESULTS AND DISCUSSIONS

3.1 Thermogravimetric Analysis (TGA)

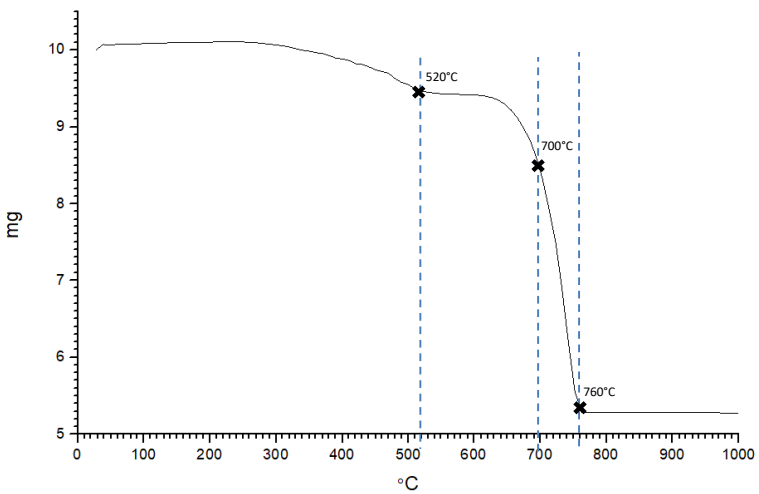

Figure 1: TGA data for raw eggshell powder

Figure 1 shows the TGA of raw eggshells. The analysis indicates a total weight loss of approximately 5% as the temperature rose from room temperature to 1000°C, which occurred in two main stages. An initial

1% weight loss up to 400°C is likely due to the evaporation of moisture and volatile organic matter. A significant 4% weight loss between 400°C and 800°C corresponds to the thermal decomposition of calcium carbonate ($CaCO_3$), releasing carbon dioxide (CO_2) and leaving calcium oxide (CaO) as a residue. The plateau after 700°C suggests the complete decomposition of $CaCO_3$. The curve also helps determine the optimal calcination temperature, around 800°C or higher, to achieve pure CaO [25]. Hence, 700°C was chosen for the calcination process to prevent the eggshell from being converted into CaO at a temperature later than 700°C [26].

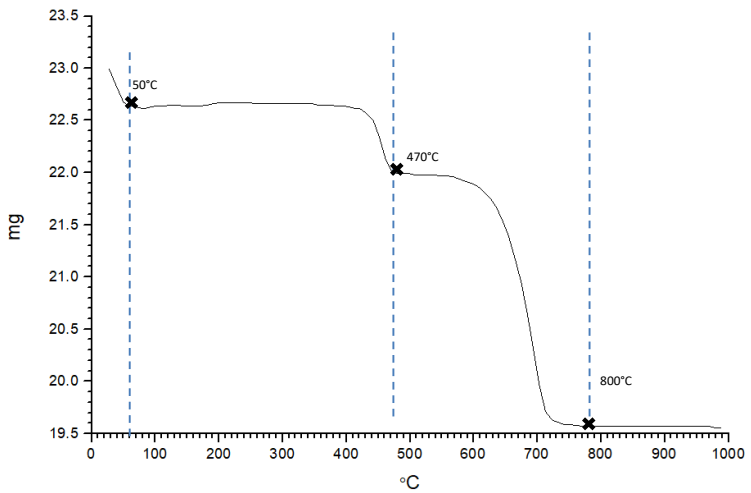

Figure 2: TGA data for ball-milled powder mixture of DCPD and calcined eggshells

In the meantime, the raw eggshell's TGA curve mixed with dicalcium phosphate dihydrate (DCPD) in Figure 2 shows a total weight loss of approximately 5% from room temperature to 1000°C. The initial gradual weight loss of about 2% up to 600°C is likely due to the evaporation of moisture, volatile organic matter, and the dehydration of DCPD into anhydrous dicalcium phosphate. The major weight loss of around 3% between 600°C and 760°C is attributed to the thermal decomposition of $CaCO_3$ in the eggshell, releasing CO_2 and forming CaO). After 800°C, the weight loss plateaud, indicating the complete decomposition of $CaCO_3$. This change suggests that the eggshell is relatively pure, as the total weight loss closely matches the theoretical 44% for pure $CaCO_3$ decomposition [25]. This TGA curve confirmed

the choice in selecting 800 °C as the optimal sintering temperature for the powder mixture to be fully converted into HA. Besides that, a higher sintering temperature than 800°C during initial HA powder preparation was reported to produce and cultivate α-TCP in the HA phase [25-27].

3.2 X-Ray Diffraction Analysis

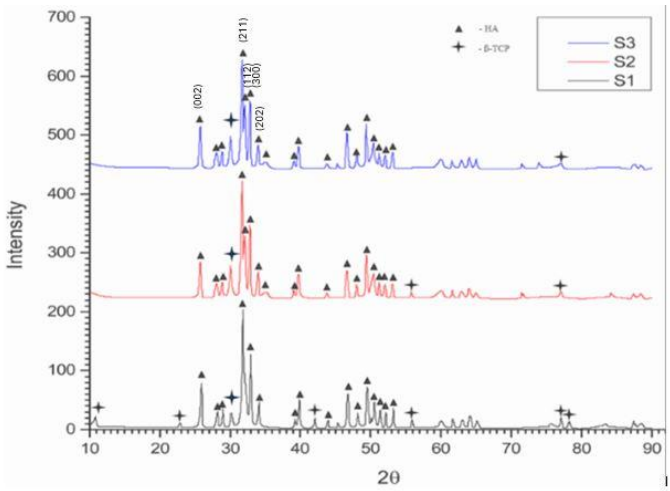

Figure 3: XRD patterns of synthesised hydroxyapatite at various ball milling times

Figure 3 shows the XRD peaks of synthesised powder prepared at different milling times. Based on the results, the synthesised powder, after heat treatment, exhibited a high degree of crystallinity in its HA content as exhibited by the peaks that belong to the HA group, which are (002), (211), (112), (300) and (202) planes. All the XRD peaks matched with the standard HA phase from JCPDS card number 01-074-9944.

However, the presence of minor β-TCP traces at 30° was found to increase as the milling times increased from 6 to 7 hours. The traces of β-TCP increased from 6 to 7 hours due to the reduction of phase stability of HA phase which then result in increased of β-TCP phase. This similar observation of HA with traces of β-TCP formation was reported by Shih-Ching Wu [28] despite the different ball-milling speeds (170 rpm) and ball-milling times (1, 5 and 10 hours) employed. However, in that work, the increasing value of ball-milling time

resulted in a decrease of β-TCP traces. This result is contrary to the findings of this research, which could be attributed to the insufficient speed of the ball milling.

In addition, a significant reduction in crystallite size was observed from 5 and 6 hours of milling time. The crystallite size for the 5-hour ball-milling times produced an average crystallite size of 16.15 nm. Meanwhile, the average crystallite size for 6 and 7 hours was 12.767 nm and 12.237 nm, respectively. This decrease in crystallite size, particularly significant between 5 and 6 hours of milling, is consistent with the mechanical attrition caused by prolonged milling [28]. While smaller crystallites offer increased surface area and potentially enhanced bioactivity [3], balancing this with maintaining sufficient crystallinity is crucial. The minimal reduction in crystallite size from 6 to 7 hours suggests an optimal milling time within this range to achieve HA with a bigger surface area.

3.3 Fourier-Transform Infrared Spectroscopy (FTIR)

Figure 4 shows a consistent presence of phosphate (PO_4^{3-}) and hydroxyl (OH^-) functional groups in the HA samples at varying ball milling times of 5, 6, and 7 hours. The presence of these two functional groups confirms the successful formation of HA across all samples [29].

The vast region between 3400 and 3600 cm^{-1}, ascribed to adsorbed water and hydroxyl groups, showed a marginal rise in intensity during the milling. This implies that longer milling times could produce finer, more surface-areas HA particles, enabling more hydroxyl group exposure and water adsorption [30]. On the other hand, when the milling time increased, the strength of peaks connected to carbonate (CO_3^{2-}) groups in the 1400–1500 cm^{-1} region steadily reduced. This discovery suggests that less carbonate substitution occurs inside the HA lattice, which might be caused by carbonate species breaking down under prolonged mechanical stress.

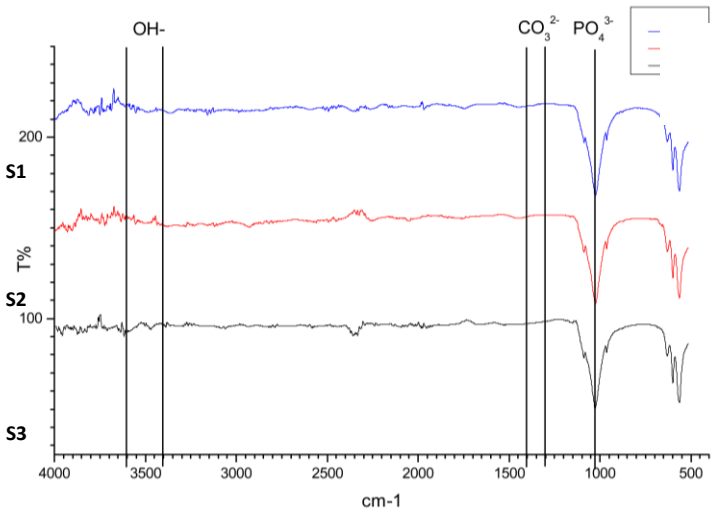

Figure 4: FTIR patterns of synthesised HA at various ball milling times

Additionally, when milling time increased, a slight shift of the primary phosphate peaks towards higher wave numbers was observed. This shift might indicate slight modifications to the phosphate environment in the HA crystal structure, possibly brought about by adjustments to bond lengths or angles due to extended mechanical activation [31]. However, these changes have not significantly influenced the overall composition of the synthesised HA.

3.4 Scanning Electron Microscopy (SEM)

Figure 5 shows the morphology of the HA with ball-milling time of 5 hours (S1), 6 hours (S2) and 7 hours (S3) under magnification of 5000X. A significant influence of milling duration on the morphological evolution and particle size was observed. The 5-hour sample exhibited a broad particle size distribution with significant agglomeration, consisting of globular-shaped fused particles. Extending the milling time to 6 and 7 hours resulted in a more homogeneous particle size distribution, with a higher proportion of smaller, rounded particles. It can be seen that the agglomeration of the particle was reduced as the milling time increased. In addition, it was found that the average particle size for 5 hours of ball-milling time was between 1.4286 - 6.7857μm.

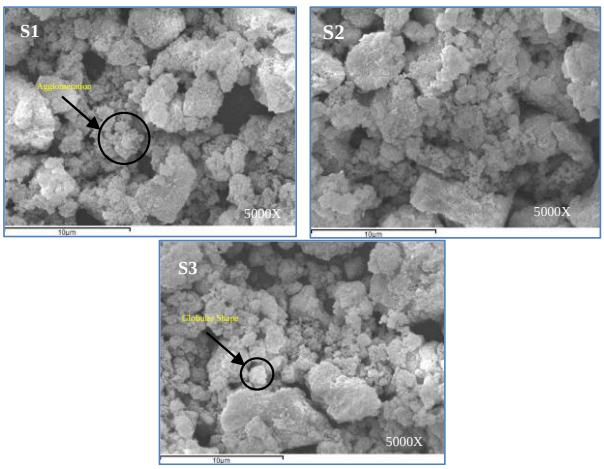

Figure 5: SEM images of synthesised HA at various ball milling times

In comparison, the particle size for 6 and 7 hours of ball-milling time was around 1.0714 - 7.857μm and 0.7143 - 6.4286μm, respectively. A similar trend was also observed in the crystallite size of the synthesised powder through the XRD analysis, where the crystallite size decreased with the increase of milling times. Besides that, the reduction in the tendency for powder agglomeration indicates that prolonged milling effectively breaks down larger particles and promotes better particle dispersion [28], [32]. The relationship between crystallite size and particle size can be observed when the ball-milling time increases; both the crystallite and particle size are reduced.

3.5 Energy Dispersive X-Ray (EDX)

Table 2: Atomic percentage of calcium and phosphorus in synthesised HA at various ball milling times

Sample	Atomic % (Ca)	Atomic % (P)	Ca/P
S1	25.00	14.29	1.749
S2	23.18	13.28	1.745
S3	22.20	14.35	1.547

Table 2 shows the EDX analysis of the ball-milled samples which indicates the presence of calcium (Ca) and phosphorus (P). It is essential for forming hydroxyapatite (HA), the main mineral component of bone. From the results, the Ca/P ratio can be calculated, and the value of the Ca/P ratio for 5 hours was 1.749. The Ca/P ratio for

6 hours was 1.745, while the Ca/P ratio for 7 hours was 1.547. The slight discrepancy in calculated Ca/P ratios to the stoichiometric ratio of 1.67 [25] for pure HA could be due to secondary phase formation in the synthesised HA, which is the minor presence of β-TCP in the samples.

CONCLUSION

HA has been successfully produced via mechanical activation at different ball milling times (5, 6 and 7 hours) and subsequent sintering regimes at 800 °C. The XRD results of all synthesised powders exhibited a high degree of HA crystallinity, with the increased presence of minor β-TCP traces as the milling times increased from 6 to 7 hours. Besides that, better crystallite size with increased milling times was observed with the values of 16.15nm, 12.767nm and 12.237nm for 5,6 and 7 hours of ball-milling time, respectively. A similar trend was also exhibited in morphological analysis whereby the agglomeration of particles along with average particle size decreased with milling times. It can be deduced that the 6 to 7 hours ball milling times, which caused a significant reduction in HA powder size, could be suggested as the range of efficient milling time. Besides that, the Ca/P ratio obtained in all synthesised powders showed a close resemblance to the Ca/P ratio of pure HA at 1.67. Thus, $CaCO_3$ from calcined eggshell waste has been successfully employed as a sustainable calcium precursor in producing HA.

ACKNOWLEDGMENTS

The authors acknowledge Institut Pengajian Siswazah Universiti Teknologi MARA (UiTM) for funding under the Conference Support Fund (CSF) and would like to thank the Faculty of Mechanical Engineering, Universiti Teknologi MARA (UiTM), Shah Alam for providing research facilities.

AUTHOR CONTRIBUTIONS

The authors confirm the equal contribution in each part of this work. All authors reviewed and approved the final version of this work.

CONFLICTS OF INTEREST

The manuscript has not been published elsewhere and is not under consideration by other journals. All authors have approved the review, agree with its submission and declare no conflict of interest on the manuscript.

REFERENCES

[1] K. M. Agarwal, P. Singh, U. Mohan, S. Mandal, and D. Bhatia, "Comprehensive study related to advancement in biomaterials for medical applications," *Sensors International*, vol. 1, Jan. 2020.

[2] M. Malakauskaite-Petruleviciene, Z. Stankeviciute, G. Niaura, A. Prichodko, and A. Kareiva, "Synthesis and characterisation of sol-gel derived calcium hydroxyapatite thin films spin-coated on silicon substrate," *Ceramics International*, vol. 41, no. 6, pp. 7421–7428, Jul. 2015.

[3] S. Ramesh *et al.*, "Characteristics and properties of hydoxyapatite derived by sol–gel and wet chemical precipitation methods," *Ceramics International*, vol. 41, no. 9, pp. 10434–10441, 2015.

[4] S. Ebrahimi, C. S. S. Mohd Nasri, and S. E. Bin Arshad, "Hydrothermal synthesis of hydroxyapatite powders using Response Surface Methodology (RSM)," *PLoS One*, vol. 16, no. 5, 2021.

[5] X. Ma, Y. Chen, J. Qian, Y. Yuan, and C. Liu, "Controllable synthesis of spherical hydroxyapatite nanoparticles using inverse microemulsion method," *Materials Chemistry and Physics*, vol. 183, pp. 220–229, 2016.

[6] J. S. Cho and S. H. Rhee, "Formation mechanism of nano-sized hydroxyapatite powders through spray pyrolysis of a calcium phosphate solution containing polyethylene glycol," *Journal of the European Ceramic Society*, vol. 33, no. 2, pp. 233–241, 2013.

[7] A.B. Hadzley, A.A. Afuza, T. Norfauzi, U.A.A. Umar, and S.G. Herawan, "Comparison of wear performance between alumina and alumina-zirconia cutting tools at higher cutting speed", Journal of Advanced Manufacturing Technology, vol. 14, no. 2 (2), pp. 137-148, 2020.

[8] N. Ahmad Nawawi, F. A. Azmi, A. Azizan, and T. B. Le, "Densification of Calcium Phosphate from Biogenic Waste for Biomedical Application," *Malaysian Journal of Medicine and Health Sciences*, vol. 19, no. s18, pp. 9–14, 2023.

[9] M. S. Firdaus Hussin, H. Z. Abdullah, M. I. Idris, and M. A. Abdul

Wahap, "Extraction of natural hydroxyapatite for biomedical applications—A review," *Heliyon*, vol. 8, no. 8, 2022.

[10] J. Vicente, C. Neto, A. Beatriz, V. Teixeira, A. Cândido, and D. Reis, "Hydroxyapatite coatings versus osseointegration in dental implants: A systematic review."

[11] A. Rajabnejadkeleshteri, A. Kamyar, M. Khakbiz, Z. L. bakalani, and H. Basiri, "Synthesis and characterisation of strontium fluor-hydroxyapatite nanoparticles for dental applications," *Microchemical Journal*, vol. 153, p. 104485, 2020.

[12] H. Shi, Z. Zhou, W. Li, Y. Fan, Z. Li, and J. Wei, "Hydroxyapatite based materials for bone tissue engineering: A brief and comprehensive introduction," *Crystals*, vol. 11, no. 2, pp. 1–18, 2021.

[13] N. Safitri, N. Rauf, and D. Tahir, "Enhancing drug loading and release with hydroxyapatite nanoparticles for efficient drug delivery: A review synthesis methods, surface ion effects, and clinical prospects," *Journal of Drug Delivery Science and Technology*, vol. 90, p. 105092, 2023.

[14] S. Ogawa, T. Sato, and M. Katoh, "Enhancing pyromorphite formation in lead-contaminated soils by improving soil physical parameters using hydroxyapatite treatment," *Science of the Total Environment*, vol. 747, p. 141292, 2020.

[15] J. Jeong, J. H. Kim, J. H. Shim, N. S. Hwang, and C. Y. Heo, "Bioactive calcium phosphate materials and applications in bone regeneration," *Biomaterials Research*, vol. 23, no. 1, 2019.

[16] T. Iwamoto, Y. Hieda, and Y. Kogai, "Effect of hydroxyapatite surface morphology on cell adhesion," *Materials Science and Engineering C*, vol. 69, pp. 1263–1267, 2016.

[17] K. A. Hing, S. M. Best, K. E. Tanner, W. Bonfield, and P. A. Revell, "Mediation of bone ingrowth in porous hydroxyapatite bone graft substitutes," *Journal of Biomedical Materials Research Part A*, vol. 68, no. 1, pp. 187–200, 2004.

[18] M. Sirait, K. Sinulingga, N. Siregar, and R. S. D. Siregar, "Synthesis of hydroxyapatite from limestone by using precipitation method," in *Journal of Physics: Conference Series*, p. 012058, 2020.

[19] M. Sadat-Shojai, M. T. Khorasani, E. Dinpanah-Khoshdargi, and A. Jamshidi, "Synthesis methods for nanosized hydroxyapatite with diverse structures," *Acta Biomaterialia*, vol. 9, no. 8. pp. 7591–7621, 2013.

[20] S. Adzila, I. Sopyan, S. Farius, N. Wahab, and R. Singh, "Mechanochemical Synthesis of Hydroxyapatite Bioceramics through Two Different Milling Media," *Materials Science and Nanotechnology I*, vol. 531–532, pp. 254–257, 2012.

[21] C. M. Mardziah, S. Ramesh, H. Chandran, A. Sidhu, and S. Krishnasamy, "Properties of sintered zinc hydroxyapatite bioceramic

prepared using waste chicken eggshells as calcium precursor," *Ceramic International*, vol. 49, no. 8, pp. 12381–12389, 2023.

[22] A. N. Natasha, S. Ramesh, L. T. Bang, and M. H. Koay, "Influence of calcination temperature in synthesising eggshell-derived calcium phosphate," *Materials Today: Proceedings*, pp. 1915–1919, 2021.

[23] H. Zhou and J. Lee, "Nanoscale hydroxyapatite particles for bone tissue engineering," *Acta Biomaterialia*, vol. 7, no. 7, pp. 2769–2781, 2011..

[24] H. Aguiar, S. Chiussi, M. López-Álvarez, P. González, and J. Serra, "Structural characterisation of bioceramics and mineralised tissues based on Raman and XRD techniques," *Ceramic International*, vol. 44, no. 1, pp. 495–504, Jan. 2018, doi: 10.1016/j.ceramint.2017.09.203.

[25] C. Rodriguez-Navarro, E. Ruiz-Agudo, A. Luque, A. B. Rodriguez-Navarro, and M. Ortega-Huertas, "Thermal decomposition of calcite: Mechanisms of formation and textural evolution of CaO nanocrystals," *American Mineralogist*, vol. 94, no. 4, pp. 578–593, 2009, doi: 10.2138/am.2009.3021.

[26] N. Binti and A. Nawawi, "Properties of Calcium Phosphate Bioceramic Prepared by Solid State and Chemical Route", Doctoral dissertation, University of Malaya.

[27] N. A. Nawawi, F. A. Azmi, A. Azizan, and L. T. Bang, "Densification of Calcium Phosphate from Biogenic Waste for Biomedical Application," *Malaysian Journal of Medicine and Health Sciences*, vol. 19, no. SUPP18, pp. 9–14, 2023.

[28] S. C. Wu, H. C. Hsu, S. K. Hsu, Y. C. Chang, and W. F. Ho, "Synthesis of hydroxyapatite from eggshell powders through ball milling and heat treatment," *Journal of Asian Ceramic Societies*, vol. 4, no. 1, pp. 85–90, Mar. 2016, doi: 10.1016/j.jascer.2015.12.002.

[29] P. Surya, A. Nithin, A. Sundaramanickam, and M. Sathish, "Synthesis and characterisation of nano-hydroxyapatite from Sardinella longiceps fish bone and its effects on human osteoblast bone cells," *Journal of the Mechanical behavior of Biomedical Materials*, vol. 119, Jul. 2021.

[30] N. Jamarun, D. Amelia, Rahmayeni, U. Septiani, and V. Sisca, "The effect of temperature on the synthesis and characterisation of hydroxyapatite-polyethylene glycol composites by in-situ process," *Hybrid Advances*, vol. 2, p. 100031, 2023.

[31] I. Mobasherpour, M. S. Heshajin, A. Kazemzadeh, and M. Zakeri, "Synthesis of nanocrystalline hydroxyapatite by using precipitation method," *Journal of Alloys and Compounds*, vol. 430, no. 1–2, pp. 330–333, 2007.

[32] S. C. Wu, H. C. Hsu, S. K. Hsu, Y. C. Chang, and W. F. Ho, "Effects of heat treatment on the synthesis of hydroxyapatite from eggshell powders," *Ceramic International*, vol. 41, no. 9, pp. 10718–10724, 2015.